Tech Science Press

Eighteen-Element Antenna for Metal-Rimmed Smartphone Sub-6 GHz LTE42 Band Applications

Saqer S. Alja'Afreh[1,*], Mallak H. Alshamaileh[1], Eqab Almajali[2], Jawad Yousaf[3] and Amir Altaf[4]

[1]Electrical Engineering Department, Mutah University, Al-karak, 61710, Jordan
[2]Electrical Engineering Department, University of Sharjah, Sharjah, UAE
[3]Department of Electrical, Computer & Biomedical Engineering, Abu Dhabi University, Abu Dhabi, UAE
[4]Department of Electrical and Computer Engineering, Sungkyunkwan University, Korea
*Corresponding Author: Saqer S. Alja'Afreh. Email: Eng.saqer-jaa@mutah.edu.jo

Abstract: Due to the limited space and large mutual coupling levels, the design of sub-6 GHz massive Multi-Input Multi-Output (m-MIMO) smartphone antenna system attracts antennas' designers and engineers worldwide. Therefore, this paper presents 18-element m-MIMO antenna system that covers the long-term evolution 42 (LTE42) frequency band (3.4–3.6 GHz) for the fifth generation (5G) applications in metallic frame smartphones. The proposed array system is etched on the long sides of a metal rim of the mobile chassis symmetrically, which is electrically connected to the system ground plane with zero ground clearance. A low-profile frame of height 7 mm ($\lambda/12.3$) is symmetrically placed below & above the ground system level. The two frame parts (above/ below the ground level) are utilized separately for the implantation of the antenna elements to achieve good space exploitation and perfect pattern diversity between elements. Orthogonal feeds are used to further increase the level of the isolation where each antenna element above the ground level is fed by a 50-ohm microstrip line, and each antenna element below the ground level is fed by a 50-ohm coplanar waveguide (CPW). The proposed antenna structure is a capacitive coupled-fed open-slot antenna with a small footprint area of 12×3.5 mm^2 ($\lambda/7.2 \times \lambda/24.5$, where λ represents the free space wavelength at 3.5 GHz). A small coupling L-shaped strip provides a capacitive coupling for the proposed 5G antenna structure. To establish the contribution of the proposed 18-element m-MIMO, the prototype of the proposed system was manufactured and successfully measured. Both measured and simulated results are shown to be in good agreement. This proves that the proposed antenna provides coverage for the LTE42 band (3.4–3.6 GHz) with acceptable isolation and efficiency. Moreover, the performance of the proposed m-MIMO were further verified via channel capacity calculation and the envelope correlation coefficient (ECC) measurement. Based on that, the proposed m-MIMO is shown to provide a desirable performance for all m-MIMO parameters while it owns the largest MIMO order in mobile terminals in the open literature.

Keywords: Metal-rim; smartphone antennas; massive MIMO; 5G band

1 Introduction

After the huge success of using the MIMO technology in fourth-generation (4G) mobile communications, the fifth generation (5G) moves toward the deployment of massive MIMO (m-MIMO) technology. m-MIMO technology can further increase the channel capacity while mitigating the unfavorable effects of multi-path problems. Thus, it represents a key solution to meet the requirements of 5G technology [1]. This new technology adds an extra challenge to antennas' designers/engineers, especially, of hand-portable wireless devices. The integration of a huge number of independent antennas (>4 elements) over a small and compact size represents a big challenge. This is due to the increase of mutual coupling level as the separation distance between antenna elements decreases [2].

Unlike previous generations, 5G suggests taking the advantage of deploying both microwave bands and millimetre wave bands. The former one is called frequency range 1 (FR1), which includes sub-6 GHz bands. The latter one is called frequency range 2 (FR2), which includes selected frequency bands above 24 GHz. In light of this, many works focused on producing massive MIMO antenna systems for sub-6 GHz smartphone applications [3–30]. LTE 42 band (3.4–3.6 GHz) represents one of the well-known 5G bands, in which most of the published works proposed antenna solutions for the LTE42 band [13–30]. Several MIMO orders have been designed for sub-6 GHz applications. Fig. 1 shows that the number of publications decreases, in the current-state of-the-art, with the increase of MIMO order. To be specific, only one work has been published with a MIMO order of 16 elements [13]. The reason behind this is the limited space inside the smartphone device, in which installing a huge number of antenna elements in the smartphone will increase mutual coupling level between array elements. Therefore, isolation circuits are highly needed to decouple antenna elements.
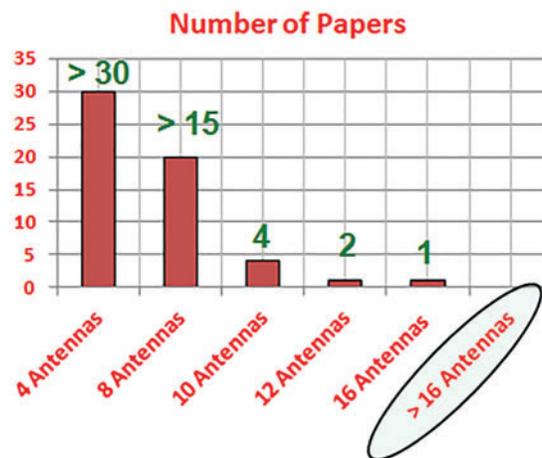

Figure 1: Survey of number of antenna elements in previous works

The open literature includes several isolation techniques, external isolation structures like protruding ground branch [3], etched slot in the ground [4,5], parasitic elements [6,7], neutralization line [5,13], have been adopted to decouple MIMO antenna elements inside mobile phones. However, they have a negative impact on the level of total efficiency. Also, the complexity of the design is normally increased. Therefore, some works have managed to overcome the aforementioned shortcoming of external isolation structures via other techniques that influence radiation mechanisms. Diversity domains like pattern diversity and polarization diversity have enabled the achievement of an acceptable level of isolation without compromising efficiency while improving channel capacity [14–16]. For the

purpose of decreasing the level of mutual coupling, sometimes space diversity is used in conjunction with pattern and polarization diversities. However, this increases the occupied space of the antenna array (large array).

Recently, various researches found that self-isolated MIMO antennas can alleviate the coupling problem. Such techniques achieve acceptable levels of total efficiency without increasing the overall size and system complexity [17–21]. This has already been proven in [20,21], as a pair of very closely spaced compact antennas (separation distance = 1.2 mm) are self-isolated by sharing a common grounding branch coupled with the two-element.

The race of sub-6 GHz massive MIMO antenna design has been started since 2015. It started with 4 × 4 MIMO antenna systems [16,20–22]. Despite these low-order arrays are effective in terms of isolation level, their channel capacity is relatively low, especially in the 5G system where the high transmission rate is extremely needed. Knowing that the ideal value of the channel capacity for a 4 × 4 MIMO array in a Rayleigh-fading channel with a 20-dB signal-to-noise ratio (SNR) is 22 bps/Hz which is almost twice the value limitation of the conventional 2 × 2 MIMO system (11.5 bps/Hz). Quadruples of the conventional state value can be obtained in an eight-element MIMO array, where the capacity upper-limit reaches 46 bps/Hz. Therefore, various published works have presented 8 × 8 MIMO arrays to operate in the long-term evolution (LTE) band 42 (3.4–3.6 GHz) [5–7,15–19,23–27]. However, one of the common drawbacks in all published works, is that they have a large modified ground plane area, which makes the integration of other smartphone components (battery, camera, and display) very difficult. Additionally, some of them like the one in [5] utilized external decoupling circuits, which degrades the total antenna efficiency as stated earlier.

Higher-order MIMO antenna systems like the 10 × 10 array have been also investigated in [9–11,29,30]. In [11], a 3.6 GHz 10 × 10 antenna MIMO array is produced. Despite the channel capacity of this array may grow up to 47 bps/Hz, the array elements are open slot radiators etched directly on the ground plane, thus the cleared ground area is substantial. The same drawback also prevails in [10,29] despite the proposed 10 × 10 antenna MIMO systems are dual-mode structures. Decoupling distributed circuits have been used between the adjacent elements in 10 × 10 antenna MIMO systems proposed in [9,29]. However, the addition of a decoupling circuit increased the complexity of the designs.

A 12-port antenna array was introduced for a dual-band 5G massive MIMO smartphone operation in [8]. The design has an acceptable diversity performance but not all elements are able to cover the lower and upper band simultaneously, in which only two-element are able to cover both frequency bands. The other 6 antenna elements are able to operate in a MIMO array at the 3.6 GHz band only, while the rest of the elements provide coverage for just the upper band (LTE 46). This justifies the reason for the low channel capacity values in both bands, which are only 34 and 26.5 bps/Hz, respectively. These rates lie below the ideal ones for an 8 × 8 MIMO system (46 bps/Hz) by about 12 and 19.5 bps/Hz in both frequency bands, respectively. In addition, the ground plane is modified on both sides such that the width of the clearance area for each element became as narrow as 3 mm. Another 12-antenna MIMO array was presented for the LTE42 band (3.4–3.6 GHz) in [14]. Despite the desirable channel capacity achieved by the array system, which is about 57 bps/Hz, the massive MIMO array is built on the upper and lower edges of the system PCB board, and the ground plane clearance is quite large of a size about 17 × 17 × 6 mm³.

In [13], a sixteen antenna MIMO array operating in the 3.5 GHz LTE42 band was proposed. The array system has been achieved using four quad-antenna linear (QAL) arrays. The achieved channel capacity for the covered band (3.4–3.6 GHz) was very attractive reaching about 66–70 bps/Hz with a

20 dB SNR ratio. However, the massive MIMO array system utilizes a 3 mm ground plane clearance on both sides. In addition, the design has relatively low total efficiency values, ranged from 30% to 52%.

According to the aforementioned state-of-the-art, it is quite clear that the current research gaps in designing massive MIMO antenna system at 3.5 GHz smartphone 5G application are: (1) There are very few works having MIMO order above 12 × 12; only the designs reported in [8,14] represent MIMO order of 12 × 12, while the work in [13] represents 16 × 16 MIMO antenna system. (2) Some massive MIMO array systems utilize at least 3 mm ground plane clearance on both long sides [8,10,13,15,23,24,28]. This reduces the allocated space for other components of the Smartphone (LCD display, battery, etc). (3) Some designs utilize parts of the upper and lower chassis edges in 5G array design [8–10,15,25,28], normally, these spaces are reserved to accommodate the LTE/WWAN antennas (2G/3G/4G antennas). (4) In [5–7,9,13,14] the reported array structures are relatively complex due to the use of external isolation circuits. To the best of our knowledge, there is no work that presents a self-isolated MIMO antenna at LTE42 band and has a mMIMO order exceeding 16 × 16 array. Thus, it is still very challenging to find a huge antenna array in a limited space for current Smartphones.

The most important contributions of this work can be summarized as follows: (1) The proposed antenna-element has a very small footprint area due to the feeding method that utilizes capacitive coupling to elements implanted on the metal rim of the smartphone. The proposed antenna structure is a coupled-fed open-slot element having many attractive characteristics; zero clearance area, low profile element (the total frame height is λ/12.3), and small footprint area (the longest dimension is λ/7). (2) the utilization of both pattern diversity (elements above and below the ground plane) and orthogonal feeds allows the installation of closely spaced elements up to nine elements on each long side of the metal rim. This allows obtaining a MIMO order of up to 18 × 18, which is not achieved yet for 5G 3.5 GHz smartphone applications.

Section 2 of the paper introduces the proposed 18 × 18 array system including its element geometry and array configuration. Section 3 presents an evolutionary process of the design and a parametric study of the effects of some vital design parameters. In Section 4, all the antennas' and MIMO performance parameters results are introduced (scattering parameters, far-field 3D radiation patterns, total radiation efficiency, channel capacity, and envelope correlation coefficient). Then the state-of-the-art comparison is introduced in Section 5. Finally, a conclusion is attached in Section 6.

2 The Proposed 18-Element Antenna System

2.1 Array Configuration

The overall geometry of the proposed 18-element MIMO antenna system is shown in Fig. 2a. A double-sided copper FR4 dielectric substrate of a 0.8 mm thickness (permittivity 4.4 and loss tangent 0.025) is used as a printed circuit board (PCB). It has overall dimensions of 80 × 150 × 0.8 mm³, which is typical for 6-inches smartphone devices. Two rectangular cleared-ground areas (80 × 5 mm) are located on the lower and upper shorter edges of the PCB. These areas are typically reserved for installing LTE/WWAN antennas (2G/3G/4G antennas). A metallic frame of 0.1 mm thickness and 7 mm height is utilized to embrace the PCB. The 7 mm height metallic frame is electrically shorted to the system's ground plane. This represents one important promising feature of this proposed design, in which the design utilizes a zero-ground plane clearance on both long sides of the PCB. Thus, the entire space is totally allocated for the LCD display and other Smartphone equipment. Such a feature is highly demanded as it is rarely achieved in the current state-of-the-art. [31]. The metallic frame height is divided into two halves: 3.5 mm below the ground plane level and 3.5 mm above the ground

plane level (the metallic frame height is symmetrical around the ground plane). This is to ensure that the overall height is about 7 mm, which is typical in real smartphones [30,31].

Figure 2: Configuration of the proposed antennas modules: (a) general view, Detailed dimensions of the proposed 5G antenna structure (b) fed by microstrip feed line, (c) fed by CPW. [Units in mm]

Due to the symmetric height of the metallic frame below & above the ground plane, the two spaces (below and above the ground plane level) are used for building two antenna groups. Pattern diversity is achieved from the existence of the system ground plane that inverts the radiation patterns in both elevation planes. Additionally, the elements of each antenna group are excited through a feeding scheme orthogonal to the feeding scheme of the other group. The etched elements on the upper portion form Group 1 (A1, A3, Ant 5, Ant 7, Ant 9 & Ant 10, Ant 12, Ant 14, Ant 16, and Ant 18) are fed by a 50-ohm microstrip feeding line each, while the etched elements on the lower portion form Group

2 (Ant 2, Ant 4, Ant 6, Ant 8 & Ant 11, Ant 13, Ant 15, and Ant 17) are fed by a 50-ohm coplanar waveguide (CPW) feeding line each. The microstrip feed line is excited through a vertically-placed 50 Ω SMA connector from the backside of the system PCB board (port Y). While in the CPW feeding method, a connector is connected horizontally (port X). For brevity, the models of connectors are hidden in Fig. 2. In light of the above information, the use of both the orthogonal feeding techniques and pattern diversity make the separation distance between any two consecutive cross-group feeds is about 15 mm, while it is about 30 mm between any two consecutive co-group feeds. This will play an important role in mutual coupling reduction as will be demonstrated later.

2.2 Antenna-Element Structure

All the proposed antenna elements (Ant 1–Ant 18) are etched on the metallic frame along the two longer sides of the system PCB. Each side has nine elements identical to the arrangement of other side's elements and distributed as follows: five elements are etched on the upper half of the frame (Group 1), while the remaining four elements are installed on the lower half of the frame (Group 2). The elements of these two groups are distributed in an alternate fashion. Figs. 2b and 2c illustrate all the details of the proposed antenna element geometry and dimensions. It can be seen that the proposed antenna structure is a compact capacitive coupled-fed open-slot antenna of area 12×3.5 mm^2 ($\lambda/7.2 \times \lambda/24.5$, where λ represents the free space wavelength at 3.5 GHz). A 0.5 mm gap is created next to the top corner of the proposed open-slot radiator structure. A matching stub is placed inside the open slot. Both the gap and the stub act as distributed capacitances. Each antenna element is coupled with an L-shaped strip. Each coupling strip for the first group is linked to a 50 Ω microstrip line, while the coupling strip for each element of the Group 2 is attached to a 50 Ω CPW feed.

3 Evolution Process and Parametric Study

This section aims to provide a detailed explanation of the design evolution process, and the effects of vital design parameters of the proposed antenna element.

3.1 Evolution Process

As shown in Figs. 3 and 4, the design process of the proposed antenna element will be illustrated by the structure evolutionary steps, and their corresponding results; reflection coefficient (S11) and input impedance, respectively.

REF1 represents an Inverted-L-shaped feeding strip that excites a small rectangular notch that is created on the metallic frame as shown in Fig. 3a. Due to the very small length of the feeding strip, its resonant frequency is above the frequency band of interest (3.5 GHz). In order to shift down the resonant frequency without increasing the modified area, an open slot is formed on the notch by creating a small gap located on the top left corner as shown in REF2. This configuration shifts resonant frequency down to 3.6 GHz (the dashed blue line in Fig. 3b). Nevertheless, REF2 impedance bandwidth is not aligned to the frequency band of interest, and even the matching level is not good at 3.5 GHz as shown in Fig. 4 (the input impedance at 3.488 GHz is: Zin = 21.5 + j 71). In order to manage this mismatching problem, an inner stub is added inside the rectangular loop to form the proposed antenna-element structure. This addition enhances the real part of the input impedance and adds capacitive impedance that equates to the inductive impedance in REF2. Thus, the proposed antenna element covers the whole band between 3.4 and 3.6 GHz (about 200 MHz bandwidth) as in Fig. 3b.
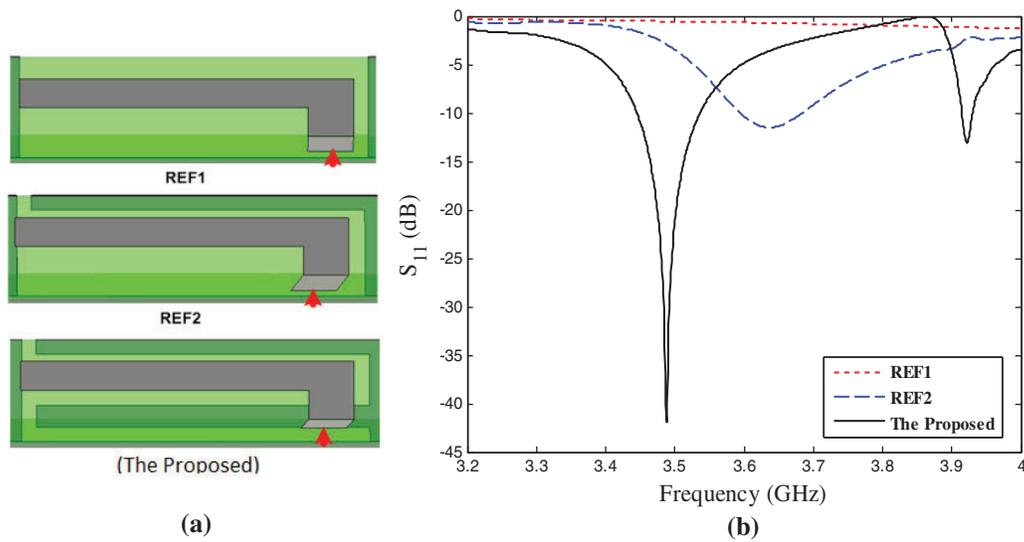
Figure 3: Antenna structure evolution steps and related reflection parameters for each; (a) Evolution of reflection parameters, (b) Antenna structure evolution
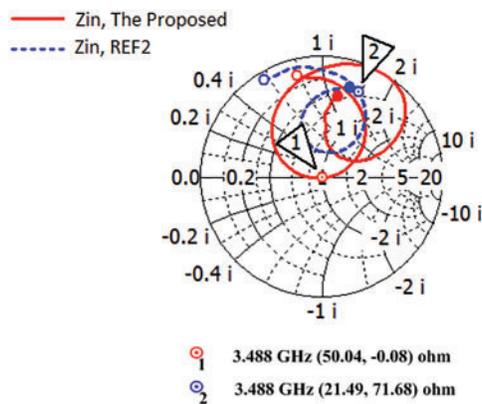

Figure 4: Simulated input impedance of REF2 and proposed antenna (Ant 5)

Fig. 5a shows the simulated current distribution resulting when Port 5 is excited, while the others are terminated with a 50 Ohms matched load each. It can be seen that due to the use of orthogonal feeds and pattern diversity among the adjacent elements of the different groups, a small coupling current reaches at Port 4 and Port 6 although their separation distances (edge to edge) from Ant 5 are very small. It can also be observed that a very small coupling current reaches the nearest antenna elements (which are Ant 3 and Ant 7), that are from the same group of Ant 5. Accordingly, the proposed MIMO antenna array does not need decoupling circuits.

Fig. 5b gives a clear view of the excited radiated mode from each antenna element. The main radiation is contributed by a quarter wavelength open-end slot. This is confirmed from the overall length of the open slot, it is about 11.5 mm, which is very near to the quarter wavelength of 3.5 GHz (free space wavelength at 3.5 GHz).
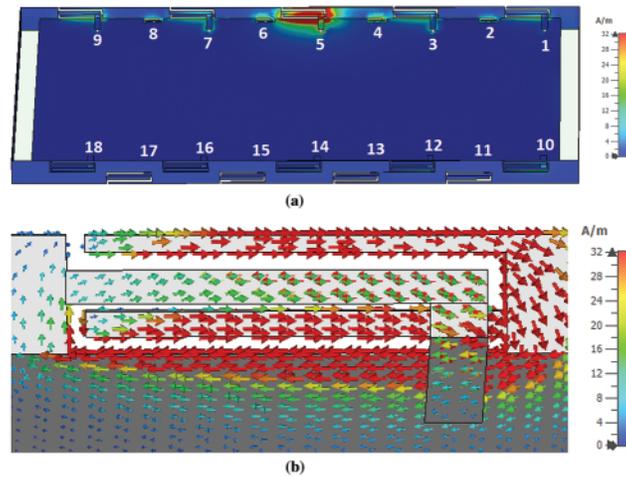
Figure 5: (a) Surface current distribution on both the system ground plane and the metal rim at 3.5 GHz, when Ant 5 is excited and others are terminated by 50 Ω, (b) Vector electric current distribution on antenna element at 3.5 GHz

3.2 Parametric Study

For an extra explanation of the working mechanism of the presented antenna, the effects of some vital structure parameters are investigated in this section. As it was clearly shown that both the gap and the stub have the main contribution to the operation of the proposed antenna-element structure, their locations and dimensions were taken into consideration very carefully to tune the results. These parameters are as follows: the position of the gap, the gap length (Lg) and finally, the stub length (Ls). It is worth noting that the other design parameters are all kept constant during the study of the effect of each aforementioned dimension separately. As the effect of these dimensions is mainly on the reflection coefficient, only the reflection coefficient results are presented. Ant 5 is chosen for this study due to the symmetry.

Fig. 6a illustrates the effect of the gap location; it has the master role in getting the desired operational band as well as a better matching level. Specifically, the resonant frequency is shifted down when the gap is located at the middle or to the right side. Also, these locations deteriorate the level matching at 3.5 GHz. Accordingly, the top left corner is selected to place the gap. This way we can obtain the desired result in terms of the best matching to cover the −6 dB bandwidth at the 3.5 GHz band.

The gap length (Lg) effect is attached in Fig.6b. it is clearly shown that the tuning of Lg affects the resonant frequency. As Lg increases the overall length of the slot decreases, and thus the resonant frequency is shifted up. Lg = 0.5 mm is chosen as the frequency band of interest is totally covered (LTE42 band 3.4–3.6 GHz) in this case. Finally, Fig.6c shows that stub length (Ls) has a similar effect as of the gap length.
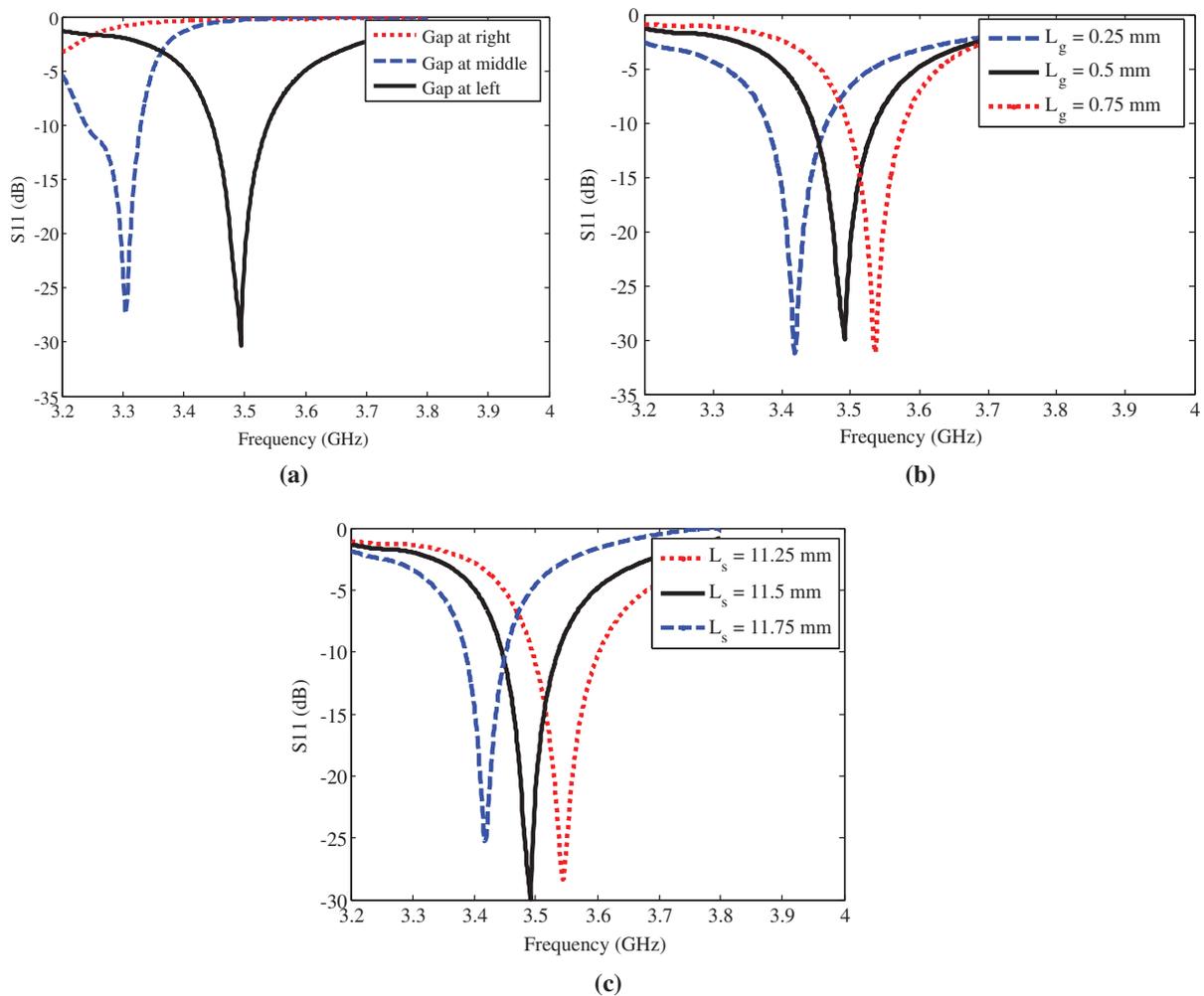
Figure 6: Parametric study results on the reflection coefficient (a) Effect of gap location, (b) effect of the gap length (Lg), and (c) effect of the stub length (Ls)

4 Simulated and Measured Results

4.1 Scattering Parameters

The proposed 18-element m-MIMO antenna has been fabricated to validate simulation results. The manufactured prototype is shown in Fig. 7. The measurement of the scattering parameter was conducted inside an anechoic chamber. The simulated and measured results of scattering parameters are shown in Figs. 8–10, in which reflection parameters results are shown in Fig. 8, while mutual coupling coefficients are shown in Fig. 9 (Co-group elements), and Fig. 10 for (cross-group). Due to the available symmetry between elements on both sides, and for the purposes of brevity, the reflection parameters result of symmetrical elements are presented in one curve. A similar trend is conducted for the mutual coupling coefficients results.

Figure 7: Fabricated Antenna prototype (a) Top view, (b) Bottom view
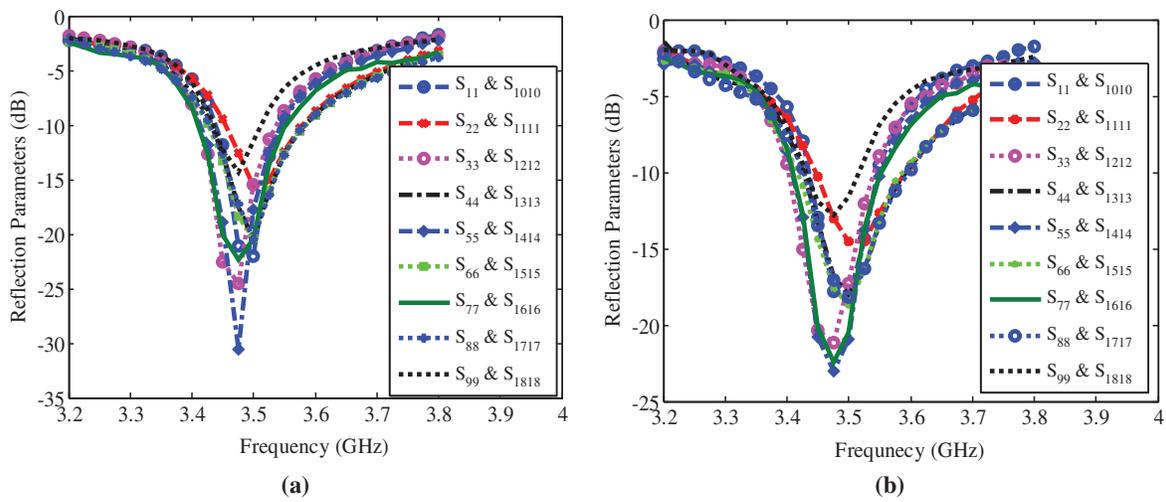

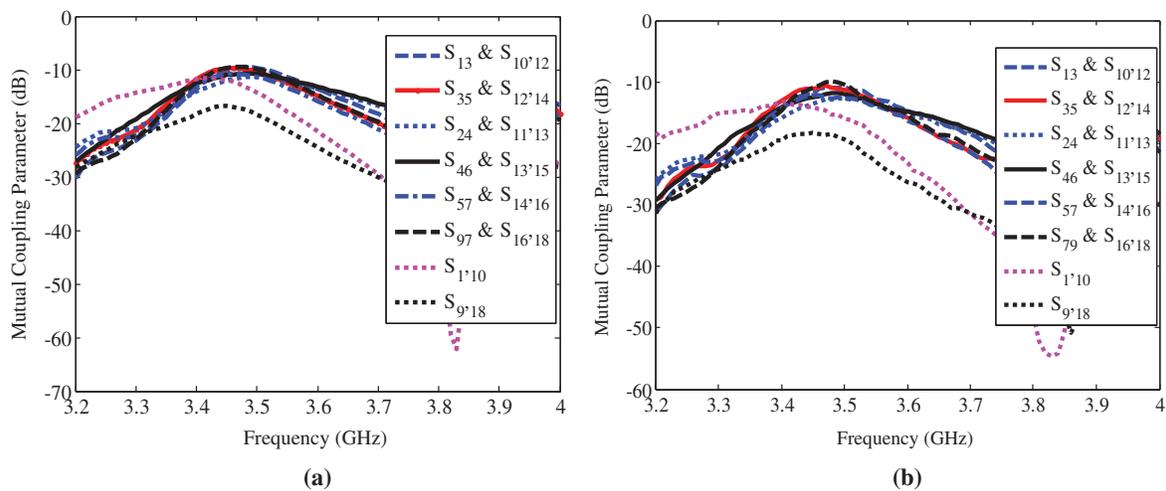**Figure 8:** Reflection coefficient (a) Simulated (b) Measured

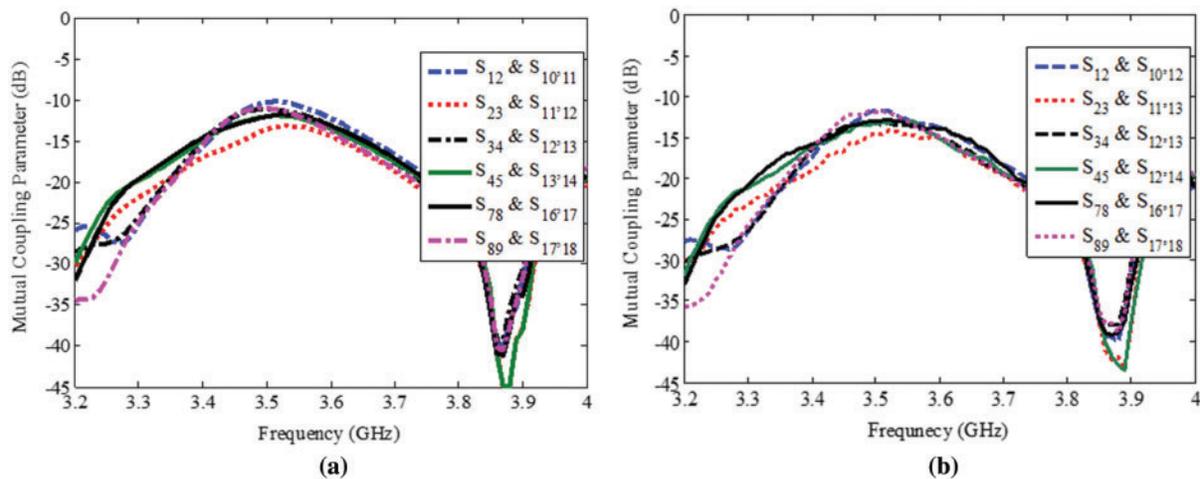**Figure 9:** Worst coupling coefficients between co-group antennas pairs (a) Simulated (b) Measured

Figure 10: Worst coupling coefficients between cross-group antennas pairs (a) Simulated (b) Measured

The simulated results of the proposed massive MIMO antenna are achieved using CST Microwave Studio [32]. Fig. 8a shows the simulated reflection coefficient of each antenna element, while Fig. 8b presents the corresponding measured ones. For the purpose of brevity, the reflection parameters of antenna elements having symmetric locations are presented in single curves. It can be noticed from both figures that both results are in good agreement. The general pattern of the curves has deep nulls around 3.5 GHz. The reflection coefficient levels of different elements are quite different from each other due to the effect of elements' location over the finite ground plane. It can be seen that the proposed antenna array has 200 MHz impedance bandwidth based on the 6 dB return loss (RL) criterion, which is the least acceptable level of RL for free space mobile phone antennas [5–10,30,31].

The simulated and the measured isolation parameters among antennas of the same group (co-group elements) are shown on Figs. 9a and 9b, respectively. Figs. 10a and 10b show the results among antenna elements of different groups (cross group elements). As the total number of isolation parameters is huge (about 289), only the results having the highest level of mutual coupling are presented in this paper to exhibit the worst case scenarios. Despite this, the mutual coupling levels are lower than −10 dB. The highest level occurs among adjacent cross-group elements like (Ant 1 & Ant 3, Ant 3 & Ant 5. etc.). The mutual coupling levels among adjacent co-group elements are below than −11 dB as the separation distance is larger than the case of adjacent cross-group elements. Overall, the measured results validate the simulated ones. This proves that the proposed MIMO antenna meets the mutual coupling criterion.

4.2 Total Radiation Efficiency

Figs. 11a and 11b show the simulated and measured results of the total radiation efficiency of the proposed 18-element m-MIMO antenna. Both results are in good correlations despite small discrepancies in some curves due to fabrication tolerances. It can be seen from both figures that the total efficiency (in free space) of the proposed antenna ranges between 45% to 70% over the entire frequency band of interest (3.4–3.6 GHz). Therefore, the proposed antenna has an acceptable total efficiency for 5G operation.
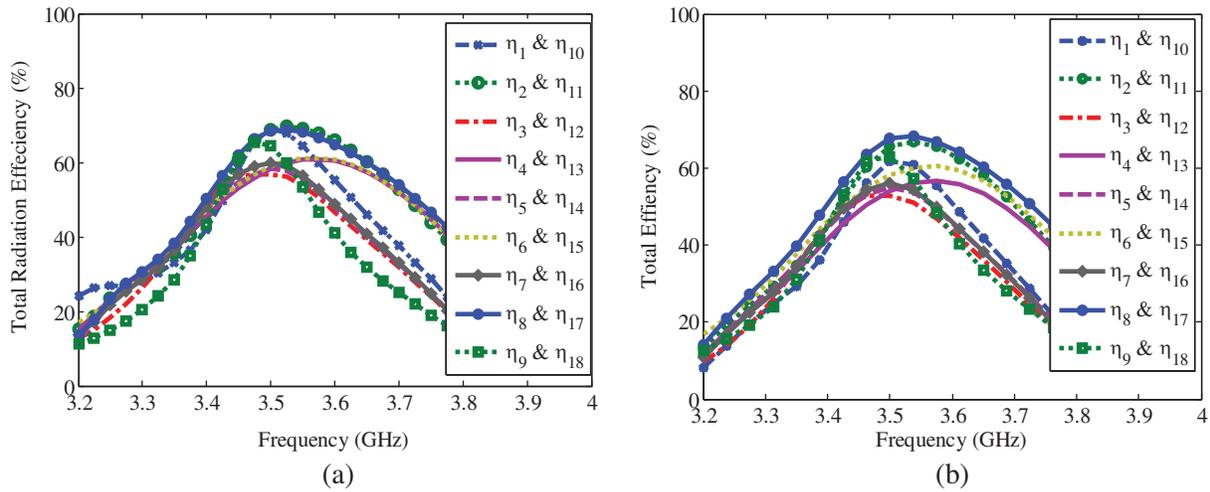
Figure 11: Total radiation antenna efficiency (a) simulated and (b) measured

4.3 Far-Field Radiation Patterns

In order to show the achieved pattern diversity among adjacent elements (Group 1 and Group 2), the simulated 3D radiation patterns at the center frequency (3.5 GHz) are shown in Fig. 12. Only the results of Antennas (Ant 1, Ant 2, Ant 3, Ant 4, Ant 5, Ant 6, Ant 7, Ant 8, Ant 9) are presented due to the limited space in this paper. The results show that the pattern diversity is clearly achieved between any two consecutive elements. As an example, Antenna 1 has complementary patterns of Antenna 2, the same can be reflected to the rest of the array's consecutive elements. This relationship gives a clear answer for the good isolation levels that are achieved in the proposed array system. Also, it ensures low levels of envelope correlation coefficient results as they will be explained in the next sub-section.

In order to validate the simulation results, the normalized far-field radiation patterns in principal planes were measured inside an anechoic chamber as shown in Fig. 13. Fig. 14 shows the simulated and measured results at 3.5 GHz of the co-polarized and the cross-polarized patterns of elements 5 in the three principal planes. Both simulated and measured results are in good agreement.

4.4 MIMO Performance Parameters

The envelope correlation coefficient (ECC) and the ergodic channel capacity represent the most important MIMO performance parameters. Therefore, this section evaluates them in free space.

The ECC represents a measure of how much received diversity signals, by two MIMO antenna elements, are different. Thus, ECC needs to be as low as possible to ensure excellent diversity performance. Practically, ECC values of below 0.5 are acceptable in recent 4G and 5G MIMO systems [30,33]. Figs. 15a and 15b show the simulated and measured ECC in free space, respectively. The calculation of both simulated and measured results is based on the 3D far-field radiation patterns, more details are available in [33]. It is worth mentioning that only the results of ECC among adjacent elements are presented, while the results of non-adjacent elements are very low so that they are not presented. It can be seen that both results are in good agreement and are below 0.15 over the frequency band of interest (3.4–3.6 GHz). Thus, the resulted diversity gain from the proposed massive MIMO antenna array will be very high and very effective in severe multipath fading channels.
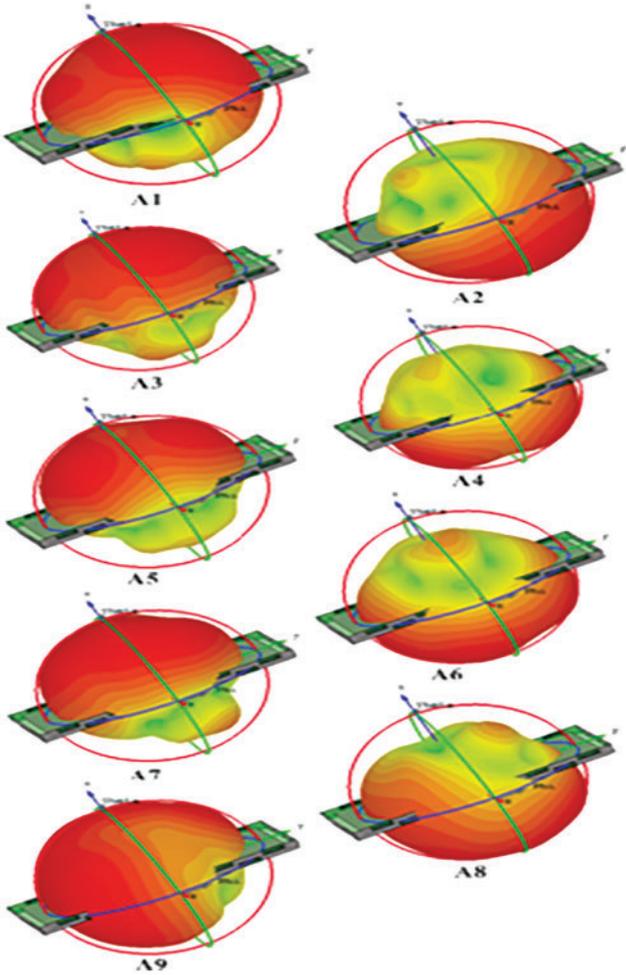
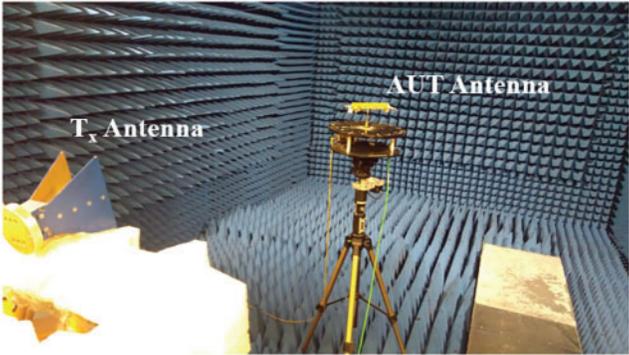**Figure 12:** 3D simulated far-field patterns at 3.5 GHz

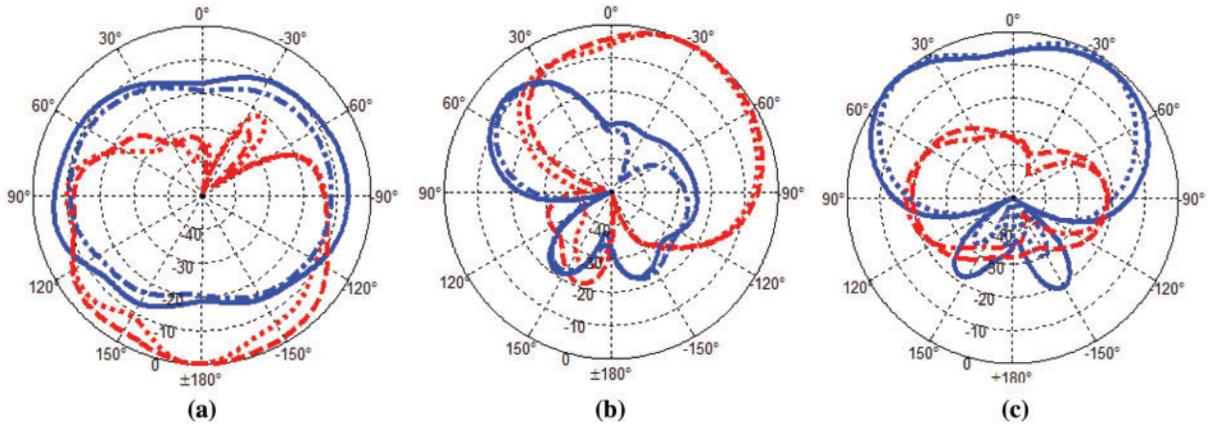**Figure 13:** Radiation patterns measurement inside Anechoic chamber

Figure 14: 2D simulated far-field patterns at 3.5 GHz. (a) XY plane, (b) XZ plane, and (c) YZ plane (Simulated Eθ in solid blue, Measured Eθ in dotted blue, Simulated EΦ in dashed red, and Measured EΦ in dashed-dotted red)
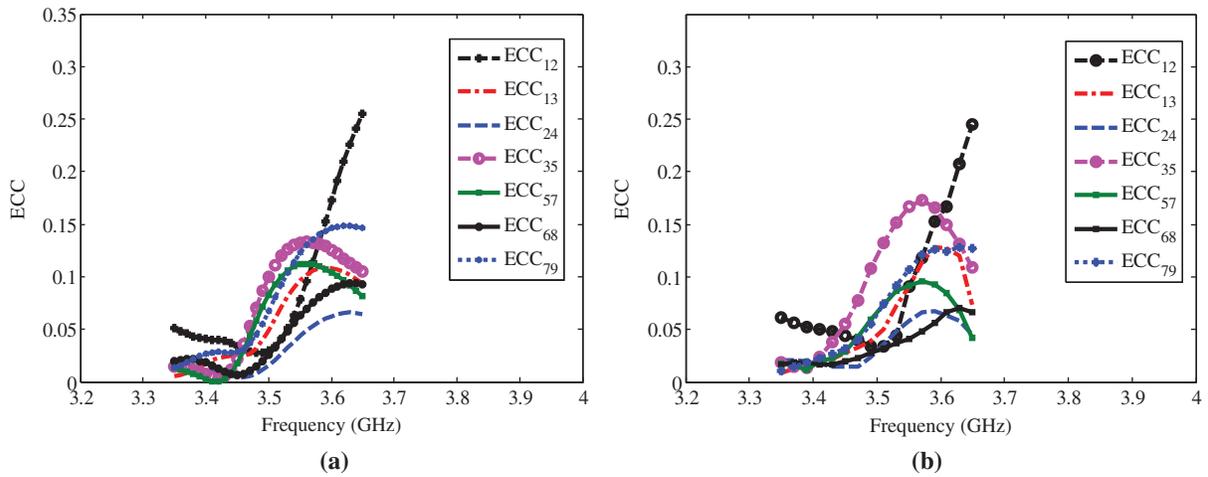

Figure 15: Envelope correlation coefficient at 3.5 GHz of (a) Simulated (b) Measured

The ergodic channel capacity (CC) is evaluated using (1) and its related equations in (2)–(4) in as in the below [30]:

$$CC = E\left\{log_2\left[det\left(I + \frac{SNR}{n}HH^T\right)\right]\right\} \tag{1}$$

The channel matric H is evaluated using

$$H = \sqrt{\varnothing_r}H_{iid}\sqrt{\varnothing_t} \tag{2}$$

The received and transmit antenna ECC matrices are calculated as follows:

$$\varnothing_r = \sqrt{\eta_{tot,r}}ECC_r\sqrt{\eta_{tot,r}} \tag{3}$$

$$\varnothing_t = \sqrt{\eta_{tot,t}}ECC_t\sqrt{\eta_{tot,t}} \tag{4}$$

where: E in (1) denotes the expectation relating to dissimilar channel realizations. I is an 18×18 identity matrix. SNR is the mean signal to noise ratio at the receiving-end array (proposed antenna array). N is the number of antennas in transmitter side, which is equal to the number of receiving antennas (N = 18). (.)T denotes the Hermitian conjugate transpose. During the channel capacity calculation, the transmitting antennas were assumed to be ideal radiators ($\eta_T = 0$) and uncorrelated ($ECC_t = 0$). The H_(i,i,d) is an 18×18 matrix, in which its entries are independent identically distributed complex Gaussian random variables.

The calculated ergodic channel capacity of the 18×18 MIMO antenna system, which is described above, is calculated from the collected measured results by averaging 20,000 independent identically distributed fading channel realization with SNR equals 20 dB [31]. As illustrated in Fig. 16, the calculated measured peak channel capacity in free space is varied between 73.2 to 82.3 bps/Hz over the whole LTE 42 frequency band. The resulting maximum channel capacity (82.3 bps/Hz) is about 79.5% of the theoretical upper limit of 18×18 MIMO antenna system in free space. With respect to SISO, it has 1431% of the upper limit of the channel capacity in SISO. Therefore, the proposed massive MIMO antenna has an excellent multiplexing performance.
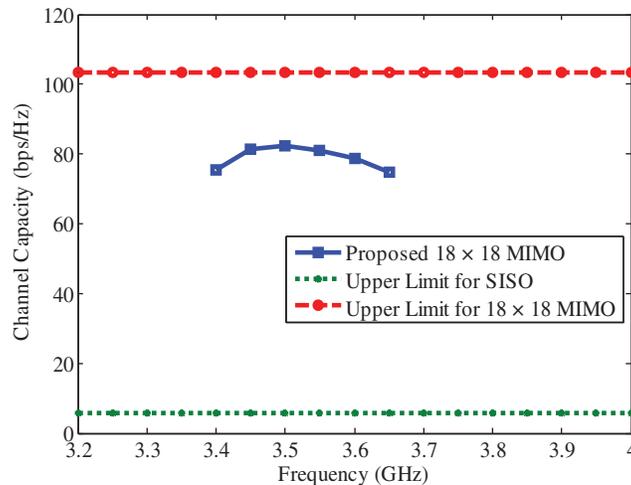

Figure 16: Measured ergodic channel capacity

5 State-of-the-Art Comparison

This section aims to introduce and summarize the values of the proposed design in comparison with other antenna solutions for Smartphone sub-6 GHz 5G massive MIMO antennas. Tab. 1 shows that the proposed design has the highest MIMO order among all published works on massive MIMO antennas; it has an order of 18 elements. Additionally, the proposed design does not consume ground plane clearance between the metal rim and the system PCB board (ground clear 0 mm). This feature simplifies the installation of other internal components (LCD display, battery, and cameras) of the smartphone without scarifying antenna performance [33]. The proposed design has an acceptable free space total radiation efficiency (greater than 45%), which is higher than half of the reported works in this paper [5,11,12,13,19]. Furthermore, the design utilizes the available space for the array in a very efficient way; this can be seen from the value of edge-to-edge spacing distance. The proposed design has the highest MIMO order as it has a very small inter-elements' edge spacing (about 3 mm) without

utilizing decoupling circuits. Finally, the design has the highest channel capacity among others (about 82.3 bps/Hz).

Table 1: Comparison between the proposed design and previous research

Ref	Bandwidth (GHz), dB	MIMO order	Ground clear (mm)	Elements edges spacing (mm)	Channel capacity (bps/Hz)	Isolation (dB)	Total efficiency (%)
[5]	3.3–3.6, −6	8	4.5	17	35	>15	>40
[10]	3.4–3.8, −6 5.1–5.9, −6	10	3	18	43.3	>11	>55
[11]	3.4–3.8, −6	10	3	20	47	>10	>42
[12]	3.4–3.6, −6	8	2	19.4	37.9	>10	>45
[13]	3.4–3.6, −6	16	3	20	70	>10	>30
[15]	2.5–2.6, −10	8	4	13.6	40	>12	>48
[17]	3.4–3.6, −10	8	0	11.2	35	>20	>60
[18]	3.4–3.6, −10	8	0	20.8	34	>19	>60
[19]	3.4–3.6, −10	8	0	15	35	>10	>40
[20]	3.4–3.6, −10	4	1	1.2	18.3	>17	>50
[21]	3.4–3.6, −10	4	1	1.2	19	>17	>55
[23]	3.4–3.6, −10	8	3	17	40	>10	>56
[28]	3.4–3.8, −6 5.1–5.9, −6	10	3	30.2	51.4	>10	>42
[This Work]	**3.4–3.6, −6**	**18**	**0**	**3**	**82.3**	**>10**	**>45**

6 Conclusion

An 18-antennas m-MIMO array operating in the LTE42 band has been presented for a 5G metal-rimmed smartphone. The proposed system has the highest MIMO order over the open literature. The MIMO array utilizes zero ground plane clearance between the metal rim and the system PCB board. One more added and selling feature of the proposed design, is a self-isolated MIMO antenna design as both patterns diversity and orthogonal feeds are used. The proposed antenna-element structure is made of a small footprint area (the longest dimension is λ/7) and a low profile (each element height is λ/24.5). It is an open-end slot excited through a capacitive L-shaped strip. Additionally, the main merit is that it's a system that introduces the array with the largest number of antennas in m-MIMO technology for the smartphone. The results show that the LTE42 band is covered under the −6 dB criterion of impedance matching, isolation level better than 10 dB without using external decoupling

circuitry, and total efficiencies are about 45%–68%. furthermore, a good MIMO performance is proven by the results of the channel capacity and ECC. Consequently, the results prove that the proposed array system is a promising solution for large channel capacity 5G massive MIMO array in metallic frame smartphones.

Conflicts of Interest: The authors declare that they have no conflicts of interest to report regarding the present study

References

[1] K. Yang, "Research and design of a high isolation 5G antenna for smart phone," in *2020 3rd Int. Conf. on Information and Computer Technologies (ICICT)*, Silicon Valley, CA, USA, pp. 507–510, 2020.

[2] M. Stanley, Y. Huang, H. Wang, S. S. Alja'afreh, Q. Xu *et al.,* "LTE MIMO antenna using unbroken metallic rim and non-resonant CCE element," in *Proc. EuCAP 2016*, Switzerland, 2016.

[3] S. S. Alja'Afreh, Y. Huang, L. Xing, Q. Xu and X. Zhu, "A low profile and wideband PILA-based antenna for handset diversity applications," *IEEE Antennas and Wireless Propagation Letters*, vol. 14, pp. 923–926, 2015.

[4] S. S. Alja'Afreh, Y. Huang and L. Xing, "A novel, low profile and wideband PIFA antenna with polarization and pattern diversities," *IET Microwaves, Antennas and Propagation*, vol. 10, no. 2, pp. 152–161, 2016.

[5] W. Jiang, B. Liu, Y. Cui and W. Hu, "High-isolation eight-element MIMO array for 5G smartphone applications," *IEEE Access*, vol. 7, pp. 34104–34112, 2019.

[6] C. -Y. -D. Sim, H. -Y. Liu and C. -J. Huang, "Wideband MIMO antenna array design for future mobile devices operating in the 5G NR frequency bands n77/n78/n79 and LTE band 46," *IEEE Antennas & Wireless Propagation Letters*, vol. 19, no. 1, pp. 74–78, 2019.

[7] W. Hu, L. Qian, S. Gao, L. -H. Wen, Q. Luo *et al.,* "Dual-band eight-element MIMO array using multi-slot decoupling technique for 5G terminals," *IEEE Access*, vol. 7, pp. 153910–153920, 2019.

[8] Y. Li, C. Sim, Y. Luo and G. Yang, "12-port 5G massive MIMO antenna array in Sub-6GHz mobile handset for LTE bands 42/43/46 applications," *IEEE Access*, vol. 6, pp. 344–354, 2017.

[9] W. Hu, X. Liu, S. Gao, L. -H. Wen, L. Qian *et al.,* "Dual-band ten-element MIMO array based on dual-mode IFAs for 5G terminal applications," *IEEE Access*, vol. 7, pp. 178476–178485, 2019.

[10] Y. Li and G. Yang, "Dual-mode and triple-band 10-antenna handset array and its multiple-input multiple-output performance evaluation in 5G," *International Journal of RF and Microwave Computer-Aided Engineering*, vol. 29, no. 2, pp. e21538, 2018.

[11] K. L. Wong and J. Y. Lu, "3.6-GHz 10-antenna array for MIMO operation in the smartphone," *Microwave and Optical Technology Letters*, vol. 57, no. 7, pp. 1699–1704, 2015.

[12] H. Zou, Y. Li, B. Xu, Y. Chen, H. Jin *et al.,* "Dual-functional MIMO antenna array with high isolation for 5G/WLAN applications in smartphones," *IEEE Access*, vol. 7, pp. 167470–167480, 2019.

[13] K. L. Wong, J. Y. Lu, L. Y. Chen, W. Y. Li and Y. L. Ban, "8-antenna and 16-antenna arrays using the quad-antenna linear array as a building block for the 3.5-GHz LTE MIMO operation in the smartphone," *Microwave and Optical Technology Letters*, vol. 58, no. 1, pp. 174–181, 2019.

[14] M. -Y. Li, Y. -L. Ban, Z. -F. Yu, J. Guo and Z. -Q. Xu, "Tri-polarized 12-antenna MIMO array for future 5G smartphone applications," *IEEE Access*, vol. 5, pp. 6160–6170, 2018.

[15] M. Y. Li, Z. Q. Xu, Y. L. Ban and Z. F. Yu, "Eight-port orthogonally dual-polarised MIMO antennas using loop structures for 5G smartphone," *IET Microwaves, Antennas & Propagation*, vol. 11, no. 12, pp. 1810–1816, 2017.

[16] L. Chang, Y. Yu, K. Wei and H. Wang, "Polarization-orthogonal co-frequency dual antenna pair suitable for 5G MIMO smartphone with metallic bezels," *IEEE Transactions on Antennas and Propagation*, vol. 67, no. 8, pp. 5212–5220, 2019.

[17] A. Zhao and Z. Ren, "Multiple-input and multiple-output antenna system with self-isolated antenna element for fifth-generation mobile terminals," *Microwave Optical Technology Letters*, vol. 61, no. 1, pp. 20–27, 2019.

[18] A. Zhao and Z. Ren, "Size reduction of self-isolated MIMO antenna system for 5G mobile phone applications," *IEEE Antennas and Wireless Propagation Letters*, vol. 18, no. 1, pp. 152–156, 2018.

[19] K. -L. Wong, Y. Tsai and J. -Y. Lu, "Two asymmetrically mirrored gap-coupled loop antennas as a compact building block for eight-antenna MIMO array in the future smartphone," *IEEE Transactions on Antennas Propagation*, vol. 65, no. 4, pp. 1765–1777, 2017.

[20] Z. Ren and A. Zhao, "Dual-band MIMO antenna with compact self-decoupled antenna pairs for 5G mobile applications," *IEEE Access*, vol. 7, pp. 82288–82296, 2017.

[21] Z. Ren, A. Zhao and S. Wu, "MIMO antenna with compact decoupled antenna pairs for 5G mobile terminals," *IEEE Antennas and Wireless Propagation Letters*, vol. 18, no. 7, pp. 1367–1371, 2019.

[22] Q. Chen, H. Lin, J. Wang, L. Ge, Y. Li *et al.,* "Single ring slot-based antennas for metal-rimmed 4G/5G smartphones," *IEEE Transactions on Antennas and Propagation*, vol. 67, no. 3, pp. 1476–1487, 2018.

[23] Y. -L. Ban, C. Li and C. -Y. Sim, "4G/5G multiple antennas for future multi-mode smartphone applications," *IEEE Access*, vol. 4, pp. 2981–2988, 2016.

[24] Y. Li, C. -Y. -D. Sim, Y. Luo and G. Yang, "High-isolation 3.5 GHz eight-antenna MIMO array using balanced open-slot antenna element for 5G smartphones," *IEEE Trans. Antennas Propagation*, vol. 67, no. 6, pp. 3820–3830, 2019.

[25] A. Ren and Y. Liu, "A compact building block with two shared-aperture antennas for eight-antenna MIMO array in metal-rimmed smartphone," *IEEE Transactions on Antennas and Propagation*, vol. 67, no. 10, pp. 6430–6438, 2019.

[26] D. Huang, Z. Du and Y. Wang, "Slot antenna array for fifth generation metal frame mobile phone applications," *International Journal of RF and Microwave Computer-Aided Engineering*, vol. 29, no. 9, pp. e21841, 2019.

[27] H. Shi, X. Zhang, J. Li, P. Jia, J. Chen *et al.,* "3.6-GHz eight-antenna MIMO array for mobile terminal applications," *AEU-International Journal of Electronics and Communications*, vol. 95, pp. 342–348, 2018.

[28] N. O. Parchin, Y. I. Al-Yasir, A. H. Ali, I. Elfergani, J. M. Noras *et al.,* "Eight-element dual-polarized MIMO slot antenna system for 5G smartphone applications," *IEEE Access*, vol. 7, pp. 15612–15622, 2019.

[29] J. Y. Deng, J. Yao, D. Q. Sun and L. X. Guo, "Ten-element MIMO antenna for 5G terminals," *Microwave and Optical Technology Letters*, vol. 60, no. 12, pp. 3045–3049, 2018.

[30] S. S. Alja'Afreh, B. Altarawneh, M. H. Alshamaileh and E. Almajali, "Ten antenna array using a small footprint capacitive-coupled-shorted loop antenna for 3.5 GHz 5G smartphone applications," *IEEE Access*, vol. 9, pp. 33796–33810, 2021.

[31] M. H. Alshamaileh, S. S. Alja'Afreh and E. Almajali, "A nona-band, hybrid antenna for metal-rimmed smartphone applications," *IET Microwaves, Antennas and Propagation*, vol. 13, no. 14, pp. 2439–2448, 2019.

[32] CST microwave studio www.cst.com.

[33] S. S. Alja'afreh, "MIMO antennas for mobile phone applications," Ph.D. Dissertation, Department of Electrical and Electronic Engineering, University of Liverpool, Liverpool, UK.